Naval Research Laboratory

Washington, DC 20375-5320

NRL/MR/6757--20-10,138

Characterizing Electromagnetic Pulses from Hypervelocity Impact Plasmas

Alex C. Fletcher

Charged Particle Physic Branch

Plasma Physics Division

February 19, 2021

REPORT DOCUMENTATION PAGE

Form Approved
OMB No. 0704-0188

1. REPORT DATE *(DD-MM-YYYY)*	**2. REPORT TYPE**	**3. DATES COVERED** *(From - To)*
19-02-2021	NRL Memorandum Report	

4. TITLE AND SUBTITLE

Characterizing Electromagnetic Pulses from Hypervelocity Impact Plasmas

5a. CONTRACT NUMBER

5b. GRANT NUMBER

5c. PROGRAM ELEMENT NUMBER
NISE

6. AUTHOR(S)

Alex C. Fletcher

5d. PROJECT NUMBER

5e. TASK NUMBER

5f. WORK UNIT NUMBER
N2M6

7. PERFORMING ORGANIZATION NAME(S) AND ADDRESS(ES)

Naval Research Laboratory
4555 Overlook Avenue, SW
Washington, DC 20375-5320

8. PERFORMING ORGANIZATION REPORT NUMBER

NRL/MR/6757--20-10,138

9. SPONSORING / MONITORING AGENCY NAME(S) AND ADDRESS(ES)

Office of Naval Research
One Liberty Center
875 N. Randolph Street, Suite 1425
Arlington, VA 22203-1995

10. SPONSOR / MONITOR'S ACRONYM(S)

NRL-NISE

11. SPONSOR / MONITOR'S REPORT NUMBER(S)

12. DISTRIBUTION / AVAILABILITY STATEMENT

DISTRIBUTION STATEMENT A: Approved for public release; distribution is unlimited.

13. SUPPLEMENTARY NOTES

Karle Fellowship

14. ABSTRACT

Projectiles that strike targets with enormous speeds will vaporize and ionize the material, producing a rapidly expanding plasma. Experiments measure electromagnetic pulses (EMPs) from sufficiently fast impacts, and the responsible physical mechanism is still not understood. We suspect that EMPs associated with meteoroid impacts are responsible for some spacecraft anomalies and failures. This project develops simulations of the production and expansion of impact plasmas. The simulations quantify the total charge generated by impacts, the plasma temperature, and plasma expansion velocity. All of these quantities agree well with ground-based experiments. We also present an outline of a planned in situ experiment which will fly either on a CubeSat or the International Space Station and will demonstrate EMPs originating from hypervelocity impacts in the theater of operation. The work detailed here is a step towards both understanding the dynamics of impact-produced plasmas as well as quantifying the threat posed to spacecraft.

15. SUBJECT TERMS

16. SECURITY CLASSIFICATION OF:			**17. LIMITATION OF ABSTRACT**	**18. NUMBER OF PAGES**	**19a. NAME OF RESPONSIBLE PERSON**
					Alex C. Fletcher
a. REPORT	**b. ABSTRACT**	**c. THIS PAGE**	Unclassified Unlimited	17	**19b. TELEPHONE NUMBER** *(include area code)*
Unclassified Unlimited	Unclassified Unlimited	Unclassified Unlimited			(202) 767-2875

Standard Form 298 (Rev. 8-98)
Prescribed by ANSI Std. Z39.18

This page intentionally left blank.

CHARACTERIZING ELECTROMAGNETIC PULSES FROM HYPERVELOCITY IMPACT PLASMAS

1. INTRODUCTION

A projectile striking a target at hypervelocity speeds will have enough energy to vaporize and ionize the projectile and part of the target material, forming a plume of dust, gas, and plasma that expands into the surrounding environment. Hypervelocity in this context is defined as a speed greater than the speed of sound of the target, which for many metals is between 5 km/s and 10 km/s. This is the speed at which a shock will form in the target and significant energy will pass into phase change and ionization [1].

The dynamics of the expanding plume of dust, gas, and plasma has received attention only in the past decade. If the expansion is into a vacuum, meaning the mean free path of the environment is significantly larger than the size of the plume, then the collective effects of the dusty plasma will govern the motion until the plume becomes sufficiently diffuse. This type of plume expansion will occur in space when a meteoroid or piece of orbital debris strikes a satellite surface, or in a ground-based impact experiment if the pressure of the chamber is low enough. Under certain conditions, impact generated plasmas will generate a burst of electromagnetic radiation, an electromagnetic pulse (EMP), as they expand. This effect has been observed in space and in ground-based impact experiments, a summary of which will follow in the next section. Fig. 1 depicts this process.

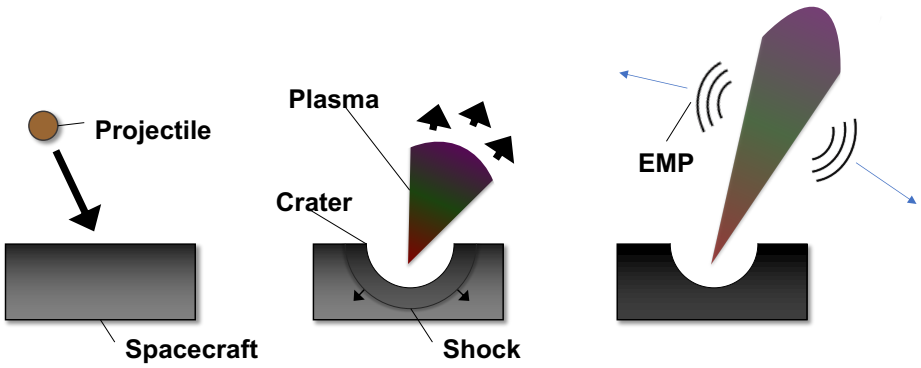

Fig. 1—Cartoon of hypervelocity with impact, plasma formation, plasma expansion into vacuum, and generation of an EMP.

The prevailing physical mechanism responsible for the EMP was put forth by Close et al. [2]. The plasma forms at near-solid densities, which is highly collisional. The expansion into vacuum lowers the density by orders of magnitude. During the expansion, the collision frequency drops more rapidly than the plasma frequency, leading to a point at which the plasma frequency becomes larger. Fig. 2 shows a model of these frequencies for the expansion of a plume from a single impact. At this point, the electrons at the

Manuscript approved February 9, 2021.

edge of the plume are free to move out ahead of the ions due to higher mobility. A macroscopic ambipolar electric electric field forms between the species, pulling the electrons back. The shell oscillates coherently for a short time and this motion creates an EMP that propagates away from the source region.

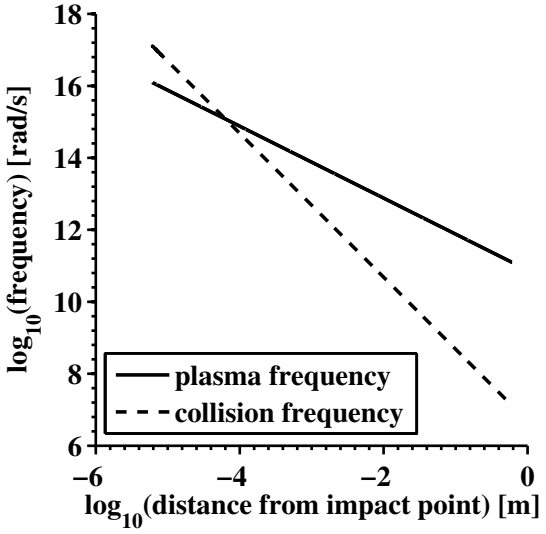

Fig. 2—The plasma and Coulomb collision frequency for an impact-produced plasma plume as it expands into the surrounding vacuum.

For faster impacts (up to 72 km/s for meteoroids) the EMP potentially has enough power to disrupt satellite electronics and interfere with sensors [3–5]. Because the EMP is an abrupt pulse and not a clean sine wave, there are a large range of frequencies making up the shape of the pulse, meaning that some of the electromagnetic energy could slip past the standard protection, like Faraday cages, present on spacecraft. The amplitude of the EMP falls off as approximately $\sqrt{1/r}$, where r is the distance from the impact point perpendicular to the velocity of the expanding plume. The total charge generated from an impact, which directly affects the power in the EMP, is a strong function of the velocity [1, 6–8], meaning that smaller, faster, and more numerous projectiles could threaten electrical damage to a spacecraft as opposed to mechanical damage.

A hypervelocity impact, including plasma formation, expansion, and radiation, is a multi-physics problem. The impact requires solid mechanics, condensed matter physics, phase change, ionization, and high energy density (HED) physics. The expansion requires both collisional and collisionless kinetic plasma physics, and free-space electromagnetic wave propagation. This process occurs over disparate time and spatial scales. Fig. 3 shows a notional impact process over a phase diagram. Modeling and simulation all of these processes at once is difficult (but possible), and ground and spaced-based experiments are critical as well.

Numerous experiments have detected plasma from hypervelocity impacts [6, 9–11]. These experiments have measured ion yields, plasma energies, temperatures, and magnetic fields associated with impacts. Further experiments have also measured radio frequency (RF) emission from impacts [12–16]. The technologies used for these experiments are usually light gas guns or electrostatic accelerators. Light gas guns produce projectiles that are slower ($\sim$10 km/s) and more massive than those on orbit, and the vacuum in the experimental chamber is insufficient to allow collective behavior of the plasma. Electrostatic accelerators

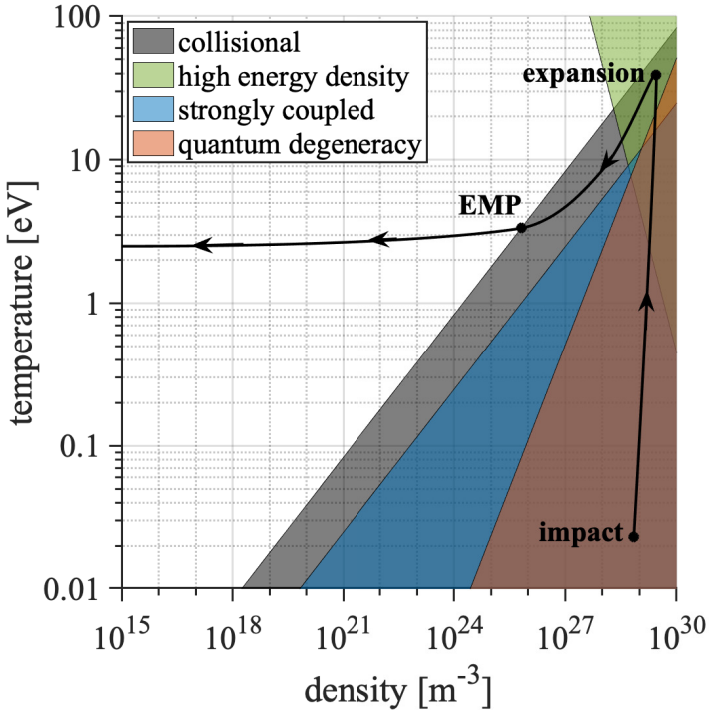

Fig. 3—Phase diagram with a notional energetic hypervelocity impact. The boundaries between different types of physics (i.e. collisional, HED, strongly coupled plasma, and quantum degeneracy) are calculated but the path of the impact plasma is qualitative.

generated projectiles at tens of km/s, but they are orders of magnitude less massive than some of the dust and debris found on orbit. Theory, simulation, and in situ measurements are thus necessary to overcome these issues inherent in ground-based impact experiments.

Numerous space missions have detected electromagnetic signals in instruments associated with impacts, even though those missions were not intended to study impacts. For instance, the Cassini spacecraft detected RF emissions from nanometer scale dust particles impacting at 450 km/s [17]. These tiny dust particles are swept up and accelerated by the solar wind. Impacts from larger particles (micrometer) traveling 10 km/s from Saturn's rings also produced RF measurements [18]. Instruments aboard the STEREO mission correlated antenna measurements with impacts using optical data [19, 20]. The Parker Solar Probe has detected hundreds of impacts with the combination of its FIELDS and WISPR instruments [21]. These impacts on the Parker Solar Probe are not yet well understood, but there are indications that the dust component of the plume may play an important role in the plasma dynamics and radiation.

Beyond chance detections of impact-associated electromagnetic emission, there have been a number of spacecraft failures that might be associated with electrical damage from an impact. These include Landsat 5 [22], Olympus-1 [23], ADEOS-II [24], and others. In many cases an impact at the time of failure was inferred, but mechanical damage from the impact was ruled out as the cause of the failures. Goel and Close [25] studied thousands of anomalies among a set of civilian satellites and found that over half were not categorizable into standard failure modes.

Section 2 of this report will discuss computational simulations of hypervelocity impact plasmas and Section 3 will discuss the design of future space-borne experiments to demonstrate EMPs from impacts in the theater of operation.

2. COMPUTATIONAL SIMULATIONS OF HYPERVELOCITY IMPACTS

As Fig. 3 demonstrates, a hypervelocity impact plasma passes through many orders of magnitude in spatial scale sizes, as well as including many different types of physics. Additionally, resolving an EMP would restrict the time scales by the speed of light while the entire impact occurs over milliseconds. This means that the temporal scales also vary over orders of magnitude. This is clearly a difficult process to simulate all at once.

In this work, we break simulations of hypervelocity impact plasmas into two parts with the first providing initial and boundary conditions for the second in a waterfall fashion. A hydrocode models the impact, solid mechanics, phase change, high energy density (HED) physics, and plasma generation, while a particle-in-cell (PIC) code takes that result into the collisionless regime to model the EMP. The basic plasma properties of the plume, such as the total charge generated, temperature, and expansion velocity, are determined by the hydrocode. The PIC takes these conditions and models any physical EMPs mechanism, kinetic instabilities, and free space radiation resulting from the impact. If the PIC is electromagnetic, this part of the simulation is severely restricted in total simulation time.

This approach is generally valid because the plasma forms from the impact (hydrocode) and separates from the target entirely, after which an EMP may be produced (PIC). One difficulty is the transition between a collisional and collisionless state in the plasma (as shown in Fig. 2. A continuum code such as a hydrocode implicitly assumes a collisional state, while PICs generally operate at their most basic level without collision between particles. PICs can include collisions through many mechanisms depending on the colliding partners [e.g. 26, 27], but these algorithms have their own restrictions and we are not aware of any that would satisfactorily model the transition regime as well. Simulations of the collisional transition are the subject of future work, and we follow the assumption of Close et al. [2] in assuming this transition is instantaneous.

In this particular report, we focus on the first part of the impact: plasma generation via impact. The code used to simulate the first stages of hypervelocity impact is ALEGRA, which was built by a team at Sandia National Laboratories [28]. At its most basic level, ALEGRA solves the continuum equations for the conservation of mass, momentum, and energy. For solid materials (i.e. projectile and target before vaporization and ionization), this requires an equation of state (EOS) to relate thermodynamic variables, a constitutive model for stresses, strains, and yielding in solids, and fracture and damage models for material failure. We used SESAME tables for the EOS and standard Johnson-Cook models for the constitutive and fracture models. These simulations incorporate phase change, which is critical for modeling the formation of hypervelocity impact plasmas, via critical density (temperature) below (above) which the phase is no longer solid. In liquid and gaseous states, the EOS is applied but stresses and strains are zero. Resolidification is not allowed in these simulations. Ionization state is determined by the LMD conductivity model [29], which incorporates pressure ionization due to HED physics. We find that pressure ionization significantly increases the ionization state in early phases of impact.

Fig. 4 shows snapshots of the mass density from six different impacts of a tungsten projectile striking an aluminum target. These materials are chosen to mimic impact experiments in which tungsten is used to

increase total charge generated due to its low work function and high density. An aluminum target would still be appropriate for a spacecraft target, while the projectile might be iron or stone for meteoroids or any number of materials for orbital debris. The six panels in Fig. 4 are for different impact speeds normal to the target surface about 12 microseconds after impact: 12 km/s, 22 km/s, 32 km/s, 42 km/s, 52 km/s, and 62 km/s. Crater formation is apparent in every case. For 22 km/s and above, there is a significant amount of gas and plasma generated that expands outwards at speeds of several km/s. Note that even for small speeds (< 8 km/s), there is still some vaporization and ionization (which is detected in light gas gun experiments). We found a threshold velocity that lies between 10 km/s and 20 km/s at which the projectile is entirely vaporized (consistent with Zel'dovich and Raizer [30]) and the plasma transitions from partially ionized to fully ionized (consistent with Fletcher et al. [1]).

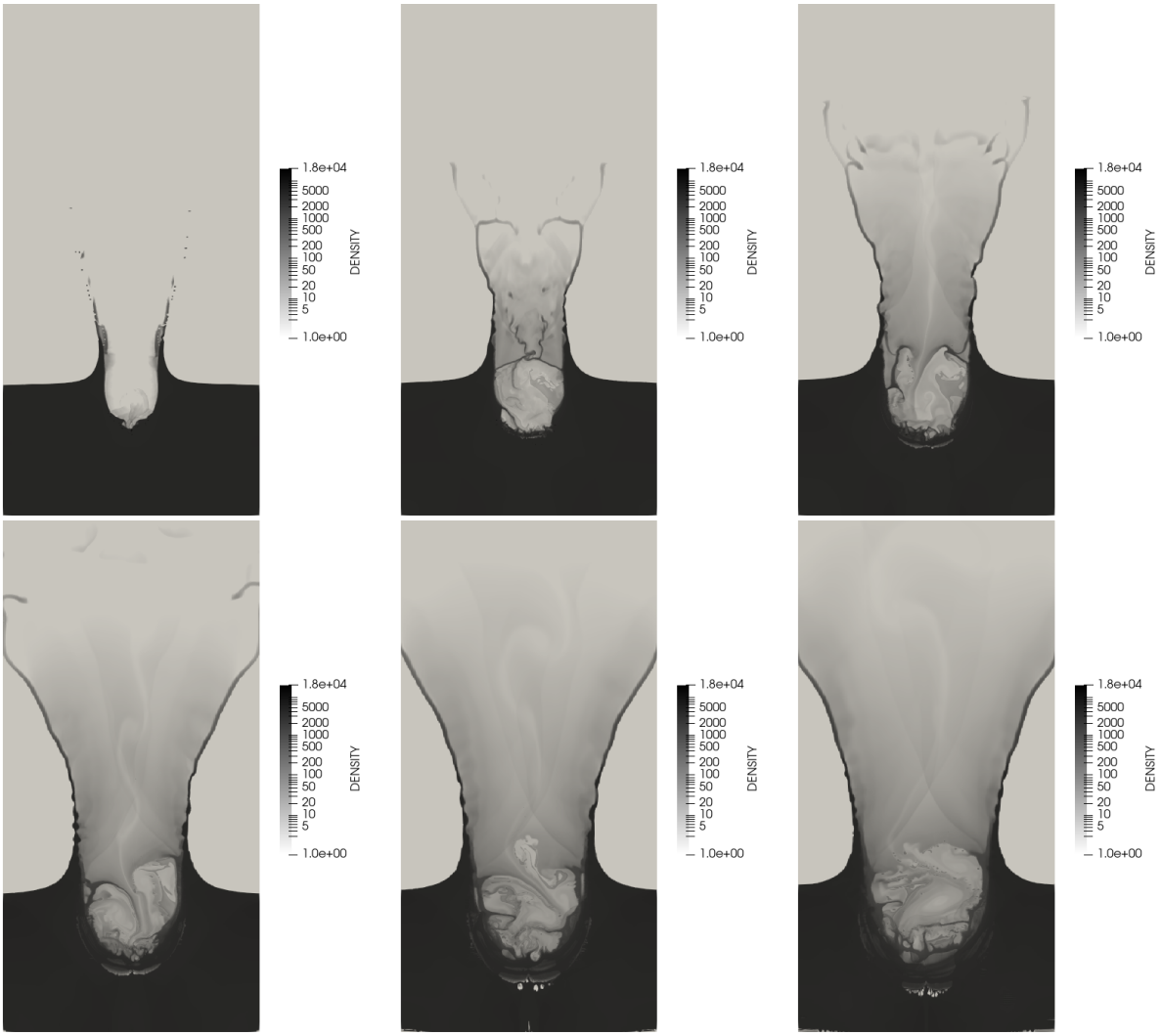

Fig. 4—Mass density snapshots approximately 12 microseconds after impact for six impact velocities: 12 km/s, 22 km/s, 32 km/s, 42 km/s, 52 km/s, and 62 km/s. The impacts are normal to the surface, the projectile is tungsten, and the target is aluminum.

Figure 5 shows snapshots of the pressure from the same six impacts from Fig. 4. It is clear that the shock wave resulting from the impact grows in intensity and speed as the impact speed increases as expected. Note

that this hemispherical shock wave is propagating through the solid material and is not the same as the craters seen in Fig. 4. Due to the Rankine-Hugoniot conditions [30], there is a limit on the jump in density across a shock and, subsequently, as the impact velocity increases, the additional energy goes into temperature (pressure). This has lead to the notion of using acoustic sensors to diagnose impacts in space (the details of the proposed experiments are in the next section). For normal impacts of known materials, two acoustic sensors near the surface of the target could measure the pressure wave seen in Fig. 5 and determine the impact location and energy. Additional acoustic sensors could determine impact angle and help constrain the mass and velocity (as opposed to just the energy) as well as constrain the material of the projectile in combination with other sensors. A full study using ALEGRA for diagnosing impacts via acoustic sensors is the subject of a future publication.

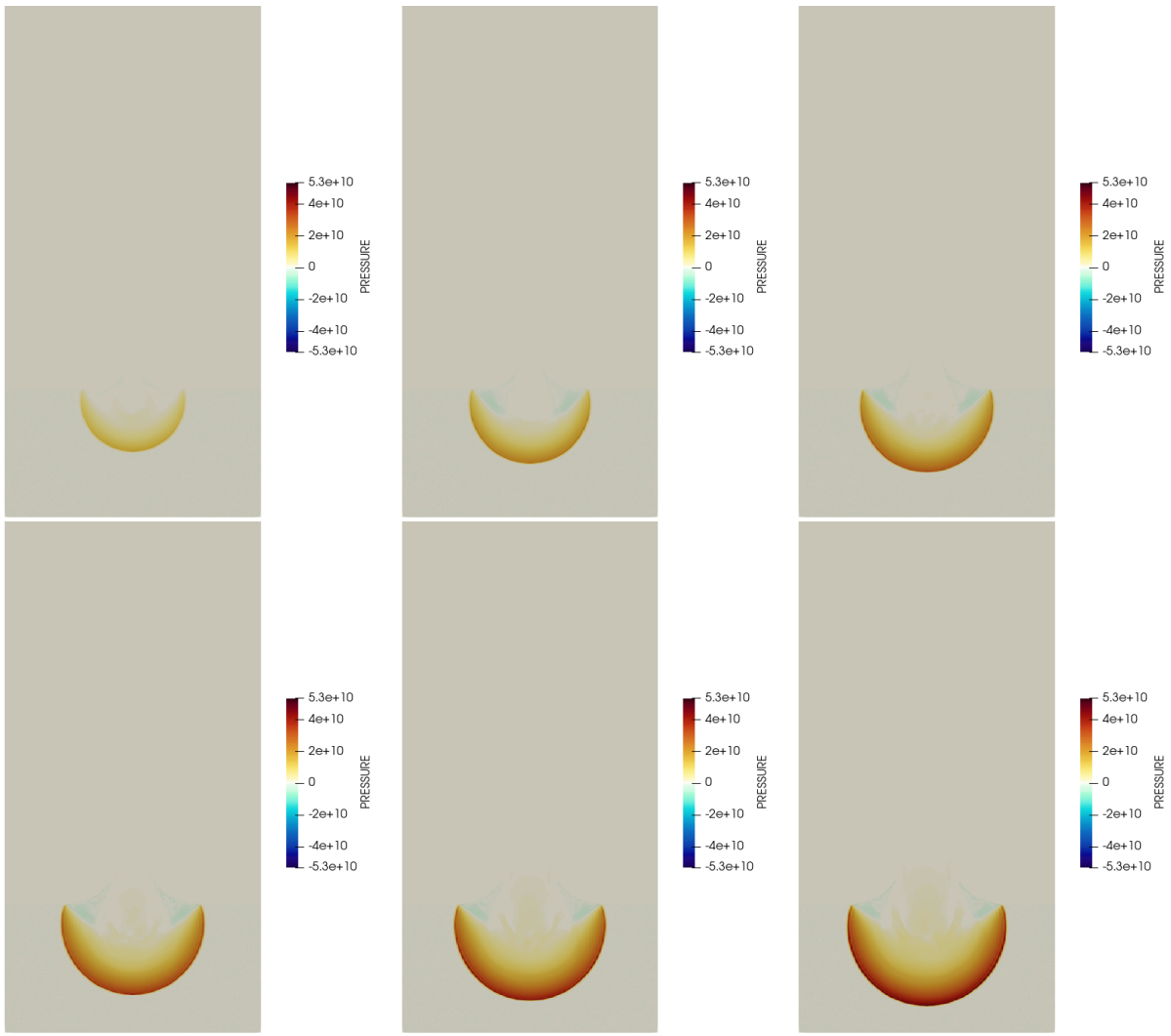

Fig. 5—Pressure snapshots approximately 2.5 microseconds after impact for six impact velocities: 12 km/s, 22 km/s, 32 km/s, 42 km/s, 52 km/s, and 62 km/s. The impacts are normal to the surface, the projectile is tungsten, and the target is aluminum.

ALEGRA also incorporates additional physics which allowed us to build significantly on the earlier simulations from Fletcher et al. [1]. Combining the magnetohydrodynamics (MHD) module with the standard

ALEGRA continuum dynamics code will provide a reduced model of the plasma effects associated with hypervelocity impacts. MHD in ALEGRA is a standard resistive MHD model. However, the limitations inherent in any MHD model (single fluid, low frequency, no free space radiation) mean that that ionization and some plasma behavior is included but the EMP mechanism and propagation is not. Fig. 6 shows an angled impact with MHD physics included. Our testing indicates that this does not change the dynamics of the plume when there is no ambient magnetic field. In the case shown here, there is a background magnetic field (which in orbit would be the Earth's magnetic field) that is parallel to the target surface before impact. The center pane (plasma density with magnetic field lines) of Fig. 6 shows how the expanding plasma distorts the background field. The left pane (density) shows both the formation of the crater and the shock wave propagating into the solid target.

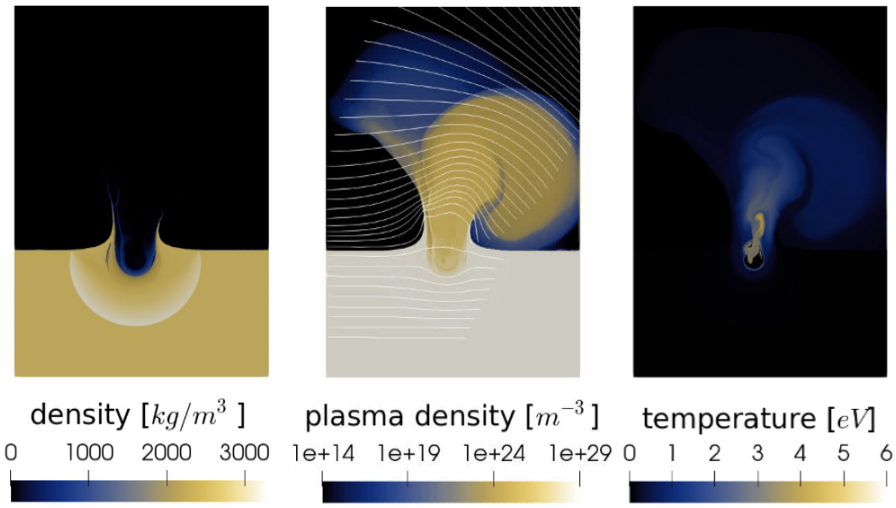

Fig. 6—A snapshot of an impact (including MHD physics) at a 30 degree angle at 30 km/s, with both materials being aluminum. The left pane is the mass density; both the formation of the crater and the shock wave propagating into the solid target are visible. The middle pane is the plasma density with the magnetic field lines drawn over; it is clear that the expanding plasma has distorted the magnetic field, which was parallel to the target surface before the impact. The right pane is the temperature, which matches well to the measured temperatures in ground-based experiments [16].

Fig. 7 shows another impact that incorporates the MHD model into the simulation. In this case, the impact is normal to the surface and the projectile is tungsten (which causes the difference in crater shape compared to Fig. 6). Another important difference is the background field, which is perpendicular to the target surface in this case. A diamagnetic cavity forms within and above the crater, creating a region of significantly reduced magnetic field strength that will collapse back to the ambient conditions as plasma density decreases due to plume expansion. This mechanism could be another source of electromagnetic fluctuations measured in-situ; in comparison to the primary EMP mechanism, the frequency content contains significantly lower frequencies and would depend critically on the configuration of the background magnetic field.

The simulations presented here are a significant improvement on previous works [1, 5], both in the realism of the material models and in the incorporated physics. While many of the simulations here were performed in a 2D cylindrical geometry, fully examining and quantifying the effects of the ambient magnetic field requires three-dimensional simulations in order to allow arbitrary magnetic field configurations (and

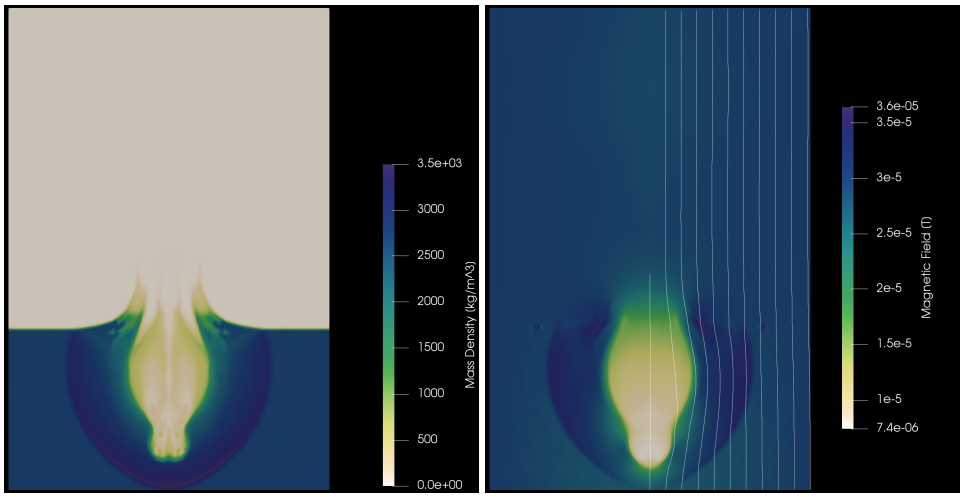

Fig. 7—A snapshot of an impact, including MHD, normal to the surface with a tungsten projectile and an aluminum target. The ambient magnetic field was perpendicular to the target surface before impact. A diamagnetic cavity forms within and above the crater, creating a region of significantly reduced magnetic field strength that will collapse back to the ambient conditions as plasma density decreases due to plume expansion.

associated arbitrary current geometries). HED physics has been incorporated via the LMD conductivity model. Experiments [16] indicate that a charged target affects the expansion of the plasma plume, and this will be included in ALEGRA simulations in the near future. Finally, hypervelocity impacts surely generated small scale dust particles (much smaller than can be resolved in these simulations), which creates a dusty plasma. There is evidence that dust ejecta could affect any emissions from hypervelocity impact plasmas [21] and need to be included in PIC simulations of impact plasma plumes.

3. SPACE-BORNE EXPERIMENTS

While ground-based impact experiments, analytic modeling, and computational simulations are useful for understanding hypervelocity impact-produced plasmas, an in situ experiment in space is necessary. Ground-based experiments cannot reproduce the projectile mass, velocity, and material regimes present in space. Light gas guns fire too few particles for useful statistics, do not have sufficient vacuum in the chamber for collisionless plasma dynamics, and cannot fire projectiles above about $\sim$10 km/s. Electrostatic accelerators do not have these difficulties, but they can only fire projectiles with a mass orders of magnitude lower than that of meteoroids and orbital debris. Simulations are possible, as seen in Sec. 2, but capturing all of the different types of physics and scales necessary at once is challenging if not impossible. Furthermore, simulations and modeling need validation via experiment. A space-borne experiment will demonstrate EMP generation from hypervelocity impacts in the theater of operation. In this section, we detail preliminary designs of an in situ experiment that would achieve this goal.

The concept of an in situ impact experiment is to essentially put target in orbit and let it be struck by impactors in the the space environment while surrounded by sensors. Fig. 8 shows the spatial density of different types of impactors on orbit averaged over the spherical shell at each altitude using ESA's Master software [31]. There are many different types of orbital debris shown as well as meteoroids. The different standard orbits are shaded and there are clear spikes in debris densities at those altitudes. The meteoroid

density changes gradually due to the combined, but opposite, effects of Earth shielding from meteoroids and attracting more meteoroids. Note this figure says nothing about the speed of the impactors, but the orbital debris pieces tend to be between 7 and 11 km/s, while the meteoroids range from 11 km/s to 72 km/s.

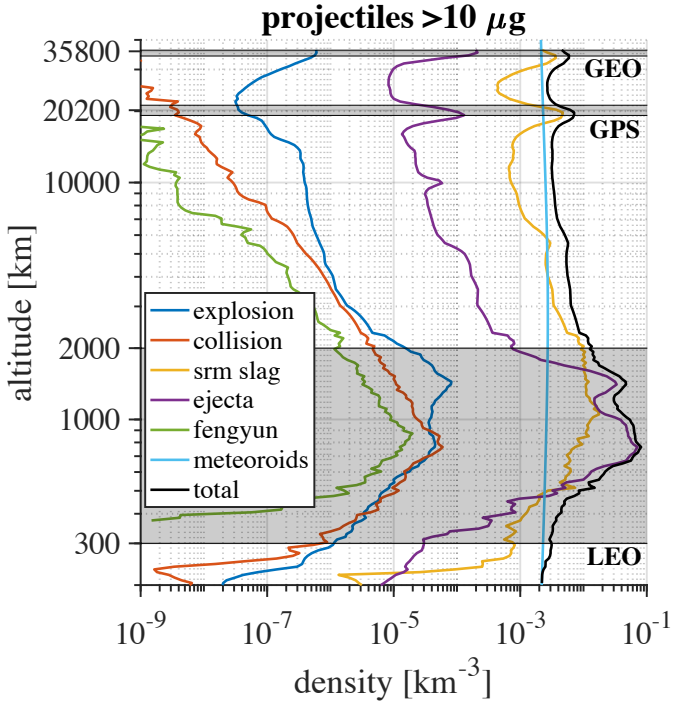

Fig. 8—Spatial density of meteoroids and different types of orbital debris, averaged over all latitudes and longitudes, as a function of altitude.

There are two clear directions for a relatively cheap in situ experiment: a CubeSat and an international space station (ISS) experiment. A CubeSat would ideally fly in the highest density altitudes of Fig. 8. However, CubeSats orbits depend on their ride to space and it is not guaranteed to get a relatively high orbit of approximately 900 km. A CubeSat might also be placed into an elliptical orbit, which would provide increased impact velocities over part of the orbit. The ISS is at approximately 420 km, where the total density is an order of magnitude lower than the peak density. An experiment on the ISS would be cheaper and simpler than a CubeSat, but would need sufficient target surface area to be struck by enough impactors to characterize the impact process over the duration of the experiment.

Fig. 9 shows two configurations of 3U CubeSats we have developed that would be capable of performing the experiment. The first (top) configuation would have solar panels deploy out from the body at an angle, with the target material underneath. The sensors, discussed below, would be on both the target and the satellite body. The second (bottom) configuration uses a deployable target, similar to a solar sail [32], to create a larger surface area (approximately 1 m^2). In this case, the sensors would have to be contained entirely on the satellite body. The first configuration would be simpler and have better diagnostics at the cost of target surface area, compared to the second configuration.

There are five sensors in Fig. 9 that would be used to characterize impact-produced plasmas and EMPs. These are similar to the experimental sensor suite used by Close et al. [16], except adapted for space.

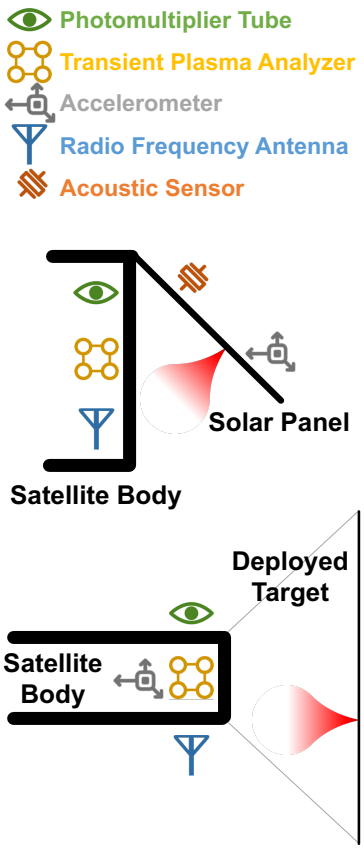

Fig. 9—Two CubeSat configurations for an in situ impact experiment.

Photomultiplier tubes would detect the visible impact flash. Accelerometers would measure changes in momentum from impacts, though they would only be effective for larger impactors. Acoustic sensors, which would not be possible in a thin deployed target, would measure the shock/sound waves that pass through the target after impact. With at least three acoustic sensors, one can reasonably diagnose the location of impact, angle of impact, and constrain the speed and mass of the impactor.

Transient plasma analyzers (TPA), which are smaller version of the standard retarding potential analyzers (RPA) [16], measure the flux of charged particles at different energies. TPAs would directly measure the impact plasma. Additionally, TPAs are the only sensor without any flight heritage and would need more extensive validation and verification than the other four sensors. Finally, radio frequency (RF) antennas would measure EMPs associated with impacts.

The choice between an ISS experiment and either CubeSat configuration depends on the cost, the flux of impactors, and the ability of the sensors to diagnose impact parameters. Fig. 10 shows the projectile flux over a year as a function of impact speed and projectile mass at an approximate circular orbit near the peak in Fig. 8 ($\sim$ 900 km). The flux was calculated using ESA's Master software [31] as well. As expected, the smaller and slower impactors are more numerous. The faster impactors ($>$ 50 km/s) are specific meteoroid showers. We estimate that an in situ impact experiment with a surface area of $\sim$1 m^2 would detect approximately one significant impact per day and several detectible but smaller impacts as well.

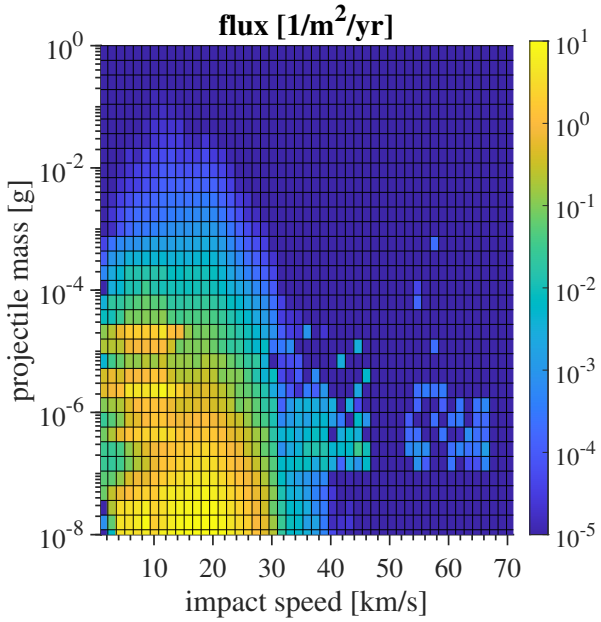

Fig. 10—Flux of impactors as a function of speed and mass over one year at an altitude of approximately 900 km.

Fig. 11 applies an experimentally determined charge generation formula [33] to look at the total plasma production from the impactors in Fig. 10. As mentioned previously, the total charge that makes up the plasma from each impact is a strong function of the velocity and scales approximately linearly with the mass [1]. We can see in Fig. 11 that the meteoroids at higher velocities will contribute significantly to the total charge generated over the mission, even though their flux is smaller. Furthermore, the scaling of the total charge generated with mass for velocities less than 50 km/s is nearly zero, so one focus would be on developing a sensor suite that can see the smaller and more numerous impacts.

This section has summarized the initial design considerations for a space-borne hypervelocity impact experiment. We argue that an impact experiment is possible in space, but the exact form (ISS or a CubeSat) will depend on further analysis of the cost and the exact flux of impactors. The analysis captured in Figs. 10 and 11 will need to be extended to several specific cases and experimental geometries. Sensor sensitivity will need to be better understood using ground-based experiments in order to know the least massive impactor that will still be detectible on orbit. Our objective is to continue the theory, computational simulation, and ground-based experiments in order to prepare for an in situ experiment in the near future.

4. CONCLUDING REMARKS

This report presents detailed hydrocode/MHD simulations of hypervelocity impact-produced plasmas in Sec. 2 and an overview of a proposed future in situ experiment in Sec. 3. The simulations indicate there is a threshold velocity between 10 km/s and 20 km/s after which the projectile is fully vaporized and the plasma becomes fully ionized as it expands in a frozen-in level of ionization. The shock wave due to the impact was modeled in order to conceive of a system of acoustic sensors embedded in the target that would be able to diagnose information from hypervelocity impacts in space. Incorporating MHD physics into impact simulations indicated that the total plasma content, expansion velocity, and temperature were

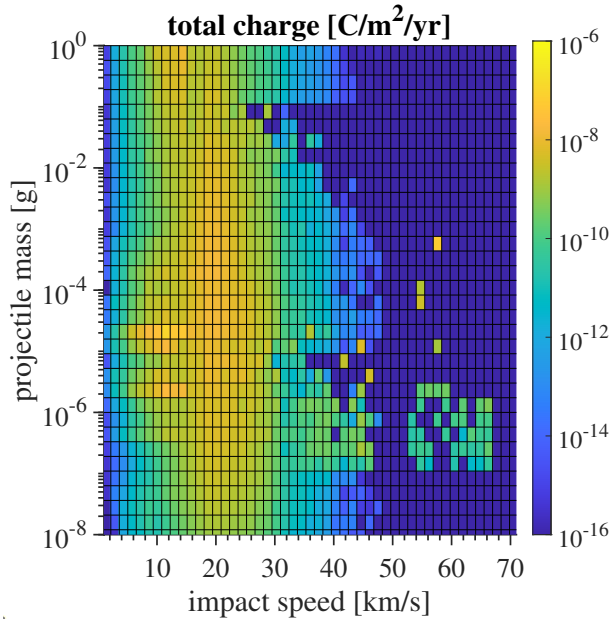

Fig. 11—Total charge generated from impactors as a function of speed and mass over one year at an altitude of approximately 900 km; calculated from the number flux in Fig. 10 and McBride and McDonnel [33].

not appreciably altered but the ambient magnetic field deformed as the plasma plume expanded away from the impact site. In certain magnetic field configurations, a diamagnetic cavity formed that leads to lower frequency electromagnetic emissions for faster impact velocities.

Because hypervelocity impact plasmas are challenging to simulate, there are many directions for future work. The use of charged targets in simulations would offer another avenue of comparison to ground-based experimental data. The most exciting step would be the incorporation of dust into the kinetic simulation of the expanding plume. This would require quantifying both the total amount of dust, the size distribution of the dust particles, and the initial velocity distribution of the dust particles. There is little question that small scale dust particles are produced by these impacts, and they are on a scale considerably smaller than what is possible to simulate with ALEGRA. Furthermore, there are hints of evidence in both ground-based impact experiments and space-borne experiments that the dust component of the plasma can have an important effect on the generation of the EMP.

We also outlined a planned experiment for demonstrating EMPs due to hypervelocity impacts in the theater of operation. This experiment would either be flown on a CubeSat with a deployable target or on the ISS. Two CubeSat configurations were presented: the first with a smaller target area and more sensors, and the second with a larger target area, fewer sensors, and a more complex deployment of the target. The ISS would likely be simpler and cheaper at the cost of particle flux due to its orbit. The overarching motivation for this program was to examine a possible threat to spacecraft that is not yet well understood. Through a combination of models, simulations, and experiments, we have estimates for the size of EMPs that could be generated by some hypervelocity impacts. A critical next step is to bridge the science from this program to an engineering analysis of the actual threat to spacecraft sensors and components.

ACKNOWLEDGMENTS

The author is grateful for the support under the Naval Research Laboratory's Karle fellowship program, as well as Gurudas Ganguli and Chris Crabtree. The simulations reported here were performed on the Centennial supercomputer at Army Research Laboratory under the Department of Defense High Performance Computing Modernization Program.

REFERENCES

1. A. Fletcher, S. Close, and D. Mathias, "Simulating plasma production from hypervelocity impacts," *Physics of Plasmas* **22**(9), 093504 (2015), doi:http://dx.doi.org/10.1063/1.4930281. URL `http://scitation.aip.org/content/aip/journal/pop/22/9/10.1063/1.4930281`.

2. S. Close, P. Colestock, L. Cox, M. Kelley, and N. Lee, "Electromagnetic pulses generated by meteoroid impacts on spacecraft," *J. Geophys. Res.* **115** (2010).

3. L. Foschini, "Electromagnetic interference from plasmas generated in meteoroids impacts," *EPL (Europhysics Letters)* **43**(2), 226 (1998). URL `http://stacks.iop.org/0295-5075/43/i=2/a=226`.

4. S. Close, M. C. Kelley, A. Fletcher, N. Lee, and P. Colestock, "RF signatures of hypervelocity impact on spacecraft," Proceedings of the 3rd AIAA Atmospheric Space Environments Conference, 2011.

5. A. C. Fletcher and S. Close, "Particle-in-cell simulations of an RF emission mechanism associated with hypervelocity impact plasmas," *Physics of Plasmas* **24**(5), 053102 (2017), doi:10.1063/1.4980833. URL `https://doi.org/10.1063/1.4980833`.

6. D. A. Crawford and P. H. Schultz, "Laboratory investigations of impact-generated plasma," *J. Geophys. Res.* **96(E3)**, 18807–18817 (1991).

7. P. R. Ratcliff, M. J. Burchell, M. J. Cole, T. W. Murphy, and F. Alladfadi, "Experimental measurements of hypervelocity impact plasma yield and energetics," *International Journal of Impact Engineering* **20**(6?10), 663 – 674 (1997), ISSN 0734-743X, doi:http://dx.doi.org/10.1016/S0734-743X(97)87453-2. URL `http://www.sciencedirect.com/science/article/pii/S0734743X97874532`, Hypervelocity Impact.

8. G. Drolshagen, "Impact effects from small size meteoroids and space debris," *Adv. Space Res.* **4(7)**(1123-1131) (2008).

9. J. F. Friichtenicht and J. C. Slattery, "Ionization associated with hypervelocity impact," *NASA-TN-D-2091* (1963).

10. D. A. Crawford and P. H. Schultz, "The production and evolution of impact-generated magnetic fields," *Int. J. Impact Engr.* **14(1-4)**, 205–216 (1993).

11. P. R. Ratcliff, M. Reber, M. J. Cole, T. W. Murphy, and K. Tsembelis, "Velocity thresholds for impact plasma production," *Adv. Space Res.* **20(8)**, 1471–1476 (1997).

12. D. A. Crawford and P. H. Schultz, "Electromagnetic properties of impact-generated plasma, vapor, and debris," *Int. J. Impact Engr.* **23(1)**, 169–180 (1999).

13. M. J. Starks, D. L. Cooke, B. K. Dichter, L. C. Chhabildas, W. D. Reinhart, and T. F. Thornhill III, "Seeking radio emissions from hypervelocity micrometeoroid impacts: Early experimental results from the ground," *Int. J. Impact Engr.* **33**, 781–787 (2006).

14. K. Maki, E. Soma, T. Takano, A. Fujiwara, and A. Yamori, "Dependence of microwave emissions from hypervelocity impacts on the target material," *Journal of Applied Physics* **97**(10), 104911 (2005), doi:http://dx.doi.org/10.1063/1.1896092. URL `http://scitation.aip.org/content/aip/journal/jap/97/10/10.1063/1.1896092`.

15. R. Bianchi, F. Capaccioni, P. Cerroni, M. Coradini, E. Flamini, P. Hurren, G. Martell, and P. N. Smith, "Radiofrequency emissions observed during macroscopic hypervelocity impact experiments," *Nature* **308**, 830–832 (1984), doi:10.1038/308830a0.

16. S. Close, I. Linscott, N. Lee, T. Johnson, D. Strauss, A. Goel, A. Fletcher, D. Lauben, R. Srama, A. Mocker, and S. Bugiel, "Detection of electromagnetic pulses produced by hypervelocity micro particle impact plasmas," *Physics of Plasmas (1994-present)* **20**(9), 092102 (2013), doi:http://dx.doi.org/10.1063/1.4819777. URL `http://scitation.aip.org/content/aip/journal/pop/20/9/10.1063/1.4819777`.

17. S. Kempf, R. Srama, M. Horanyi, M. Burton, S. Helfert, G. Moragas-Klostermeyer, M. Roy, and E. Grün, "High-velocity streams of dust origination from Saturn," *Nature* **433(7023)**, 289–291 (2005).

18. R. Srama, S. Kempf, G. Moragas-Klostermeyer, S. Helfert, T. Ahrens, N. Altobelli, S. Auer, U. Beckmann, J. Bradley, M. Burton, and et al., "In situ dust measurements in the inner Saturnian system," *Planetary and Space Science* **54(9-10)**, 967–987 (2006).

19. N. Meyer-Vernet, M. Maksimovic, A. Czechowski, I. Mann, I. Zouganelis, K. Goetz, M. Kaiser, O. S. Cyr, J. L. Bougeret, and S. D. Bale, "Dust detection by the wave instrument on STEREO: nanoparticles picked up by the solar wind?," *Solar Physics* **256(1)**, 463–474 (2009).

20. O. C. St. Cyr, M. L. Kaiser, N. Meyer-Vernet, R. A. Howard, R. A. Harrison, S. D. Bale, W. T. Thompson, K. Goetz, M. Maksimovic, J. L. Bougeret, D. Wang, and S. Crothers, "STEREO SECCHI and S/WAVES observations of spacecraft debris caused by micron-size interplanetary dust impacts," *Solar Physics* **256(1)**, 475–488 (2009).

21. J. R. Szalay, P. Pokorny, S. D. Bale, E. R. Christian, K. Goetz, K. Goodrich, M. E. Hill, M. Kuchner, R. Larsen, D. Malaspina, D. J. McComas, D. Mitchell, B. Page, and N. Schwadron, "The Near-Sun Dust Environment: Initial Observations from Parker Solar Probe," *ApJS* **256**, 2 (2020).

22. USGS, "Landsat 5 - not ready to quit yet," *Landsat Update* **3(4)** (2009).

23. R. D. Caswell, N. McBride, and A. Taylor, "Olympus end of life anomaly - a Perseid meteoroid impact event?," *Int. J. Impact Engr.* **17(1-3)**, 139–150 (1995).

24. M. Cho, "Failure mechanisms and protection methods of spacecraft power system," *Proceedings of 2005 International Symposium on Electrical Insulating Materials* **1**(45-48) (2005).

25. A. Goel and S. Close, "Electrical anomalies on spacecraft due to hypervelocity impacts," Proceedings of the Aerospace Conference, IEEE, 2015, p. 2.1104.

26. V. Vahedi and M. Surendra, "A Monte Carlo collision model for the particle-in-cell method: applications to argon and oxygen discharges," *Computer Physics Communications* **87**(1), 179 – 198 (1995), ISSN 0010-4655, doi:https://doi.org/10.1016/0010-4655(94)00171-W. URL http://www.sciencedirect.com/science/article/pii/001046559400171W, Particle Simulation Methods.

27. D. S. Lemons, D. Winske, W. Daughton, and B. Albright, "Small-angle Coulomb collision model for particle-in-cell simulations," *Journal of Computational Physics* **228**(5), 1391 – 1403 (2009), ISSN 0021-9991, doi:https://doi.org/10.1016/j.jcp.2008.10.025. URL http://www.sciencedirect.com/science/article/pii/S0021999108005615.

28. Sandia National Laboratories, "Integrated Codes: ALEGRA (2020). URL https://www.sandia.gov/ASC/integrated_codes.html.

29. M. Desjarlais, "Practical Improvements to the Lee-More Conductivity Near the Metal-Insulator Transition," *Contributions to Plasma Physics* **41**(23), 267–270 (2001), doi:10.1002/1521-3986(200103)41:2/3<267::AID-CTPP267>3.0.CO;2-P. URL https://onlinelibrary.wiley.com/doi/abs/10.1002/1521-3986%28200103%2941%3A2/3%3C267%3A%3AAID-CTPP267%3E3.0.CO%3B2-P.

30. Y. B. Zel'dovich and Y. P. Raizer, *Physics of Shock Waves and High-Temperature Hydrodynamic Phenomena* (Dover, 1966).

31. S. Flegel, J. Gelhaus, C. Wiedemann, P. Vrsmann, M. Oswald, S. Stabroth, H. Klinkrad, and H. Krag, "The master-2009 space debris environement model," *European Space Agency, (Special Publication) ESA SP* **672** (01 2009).

32. R. W. Ridenoure, R. Munakata, S. D. Wong, A. Diaz, D. A. Spencer, D. A. Stetson, B. Betts, B. A. Plante, J. D. Foley, and J. M. Bellardo, "Testing The LightSail Program: Advancing Solar Sailing Technology Using a CubeSat Platform," *JoSS* **5**(2), 531–550 (2016).

33. N. McBride and J. A. M. McDonnel, "Meteoroid impacts on spacecraft: sporadics, streams, and the 1999 Leonids," *Planet. Space Sci.* pp. 1005–1013 (1999).